Published in final edited form as:
Nat Neurosci. 2013 January ; 16(1): 13–15. doi:10.1038/nn.3284.

Neurogliaform cells dynamically regulate somatosensory integration via synapse-specific modulation

Ramesh Chittajallu, **Kenneth A Pelkey**, and **Chris J McBain**
Program in Developmental Neurobiology, Eunice Kennedy Shriver National Institute of Child Health and Human Development, National Institutes of Health, Bethesda, Maryland, USA

Abstract

Despite the prevailing idea that neurogliaform cells produce a spatially unrestricted widespread inhibition, we demonstrate here that their activity attenuates thalamic-evoked feed-forward inhibition in layer IV barrel cortex but has no effect on feed-forward excitation. The result of this circuit selectivity is a dynamic regulation in the temporal window for integration of excitatory thalamic input, thus revealing a new role for neurogliaform cells in shaping sensory processing.

The layer IV somatosensory (barrel) cortical circuit accurately encodes temporal features of tactile sensory inputs because of efficient thalamic recruitment of strong feed-forward inhibition (FFI). FFI, predominantly mediated by parvalbumin (PV)-expressing fast-spiking interneurons[1,2], imposes a restricted integration time window for summation of excitatory inputs conferring temporal precision for faithful representation of sensory information encoded in thalamic synchrony[2,3]. The subtype of interneuron termed the neurogliaform cell (NGFC) has been identified in layer IV of the barrel cortex[4]. NGFCs have axons with dense arborization containing many release sites, of which a large proportion are not associated with classical synapses resulting in GABA volume transmission[5,6]. Despite the potential of NGFCs to interact with large areas of microcircuits in a relatively target-independent manner, little is known about how NGFC activity influences neural circuit function. Here we sought to determine the role of NGFCs in layer IV barrel microcircuit with a focus on their interaction with the canonical thalamic evoked FFI.

We used transgenic mouse lines expressing $5HT_{3A}$R-GFP or NPY–humanized Renilla GFP (NPY-hrGFP) to target NGFCs in layer IV (Online Methods, Fig. 1a and Supplementary Fig. 1a–c). GFP^+ cells in either transgenic mice never express PV (Fig. 1b and Supplementary Fig. 1d–f). Layer IV NGFCs had dense axonal arborization, a late spiking phenotype and synaptic properties (Fig. 1c,d and Supplementary Fig. 2), consistent with

Correspondence should be addressed to C.J.M. (mcbainc@mail.nih.gov).

Note: Supplementary information is available in the online version of the paper.

AUTHOR CONTRIBUTIONS
R.C. conducted the experiments and data analyses. R.C., K.A.P. and C.J.M. designed the experiments. R.C. and C.J.M. wrote the manuscript.

COMPETING FINANCIAL INTERESTS
The authors declare no competing financial interests.

those described for NGFCs in other regions[6–9]. We obtained dual recordings from NGFCs and stellate cells (Fig. 1e) in a thalamus-connected layer IV barrel. Thalamic stimulation (0.1 Hz) evoked an outward current in stellate cells (Fig. 1f) that represents a $GABA_A$ receptor–mediated feed-forward inhibitory postsynaptic current (IPSC) owing to strong, effective recruitment of fast-spiking interneurons, as previously described[1,2,10]. Although we also observed an excitatory postsynaptic potential (EPSP) in the simultaneously current-clamped NGFC, it was never suprathreshold (Fig. 1f). We monitored the FFI amplitude for a baseline period (1.5 min) after which we elicited NGFC action potential firing via current injection (3 × 50 Hz for 3.5 min; Fig. 1f,g) immediately before the thalamic stimulation (Online Methods). NGFC activity resulted in unitary IPSCs on stellate cells (Fig. 1f) because of their high connectivity rate (91%; 52 of 57 NGFC–stellate cell pairs tested). However, these displayed a slower time course than the thalamic-evoked feed-forward IPSCs (Fig. 1f), demonstrating the latter was not due to NGFC recruitment. FFI amplitude was reduced after the onset of NGFC firing, which was potentiated upon block of GAT-1–mediated GABA uptake by 25 μM SKF-89976A (Fig. 1f–l) indicating involvement of extra-synaptic GABA receptors[11]. Attenuation of FFI did not persist in the face of continued NGFC activity (Fig. 1; in presence of GAT-1 block, feed-forward IPSC amplitude at 1 min and 3.5 min of NGFC activation = 39% ± 12% and 101% ± 18%, respectively; percentage of baseline, mean ± s.e.m; $P < 0.05$, Mann-Whitney U test).

A hallmark of GABA volume transmission by NGFCs is the efficient activation of $GABA_B$ receptors in the microcircuit[5,6]. Here we found that baclofen inhibited thalamic-evoked FFI (Supplementary Fig. 3a–c) and CGP55845A prevented NGFC-mediated regulation of FFI (Fig. 1j–l), demonstrating the involvement of $GABA_B$ receptor activation in the regulation of FFI. Modulation of FFI occurs during repetitive thalamic stimulation and is predominantly caused by a reduced thalamic recruitment of fast-spiking interneurons[2]. We therefore examined whether a decrease in fast-spiking interneuron recruitment, perhaps via activation of presynaptic $GABA_B$ receptors[5] that inhibit thalamocortical EPSCs on fast-spiking interneurons (Supplementary Fig. 3d–g), underlies NGFC-mediated regulation of FFI. Using a transgenic mouse expressing NPY-hrGFP and with *Nkx2-1*-driven *cre* (*Nkx2.1-cre*) activity reported by *loxP*-flanked *tdTomato* (Online Methods and Fig. 2a), we obtained simultaneous recordings (Fig. 2b) from a layer IV GFP^+ cell and $tdTomato^+$ cell with late-spiking (Fig. 1d) and fast-spiking (Fig. 2c) phenotypes, respectively. Even though transmission at this synapse was modulated by presynaptic $GABA_B$ receptors, the thalamic-evoked monosynaptic EPSC onto fast-spiking interneurons was unaltered by NGFC activity (Fig. 2d–f) under similar conditions that resulted in a robust attenuation of FFI (with GAT-1 blocked; Fig. 1h,i,l). These data suggest the locus of action for NGFC-mediated attenuation of FFI must reside in the intracortical feed-forward inhibitory circuitry of layer IV and could result from activation of presynaptic $GABA_B$ receptors at fast-spiking interneuron axon terminals that inhibit GABA release (Supplementary Fig. 3h–k).

As interaction between the direct monosynaptic excitation and disynaptic FFI on stellate cells after thalamic afferent activity is critical in determining the integration time window[2], we investigated the effect of NGFC activity on the thalamic-evoked monosynaptic EPSC onto stellate cells. We monitored the direct thalamocortical EPSC on stellate cells and

observed no inhibition of this input during NGFC firing (Fig. 2g–j) under the same experimental conditions that resulted in a robust decrease of FFI (with GAT-1 blocked; Fig. 1h,i,l and Fig. 2j). Therefore, NGFC activity selectively inhibited thalamic-evoked FFI, while leaving the monosynaptic excitation of stellate cells intact (Fig. 2j). A simple predictive model (Online Methods) linearly summing the thalamic-evoked stellate cell EPSGs and disynaptic feed-forward IPSCs, scaled according to the mean percentage change in the experimentally determined EPSCs and feed-forward IPSCs during NGFC firing (Fig. 2j and Supplementary Fig. 4a,b), demonstrated that the integration time window approximately doubled (Supplementary Fig. 4c,d) as a consequence of this specific circuit modulation.

The transient nature of the NGFC-mediated circuit modulation (Fig. 1i and Supplementary Fig. 4d) could constitute a regulatory mechanism to prevent prolonged imbalance of excitation and inhibition. A reduction in GABA release from NGFCs via activation of presynaptic $GABA_B$ autoreceptors[5,9] and/or possible desensitization of the $GABA_B$ receptors[12] responsible for FFI attenuation could underlie the transitory influence of NGFC activity in modulating the integration time window. Several mechanisms may explain the synapse-selective modulation of the layer IV circuit imparted by NGFC activity we described. Assuming a spatially uniform GABA transient in the axonal cloud upon NGFC volume transmission, selectivity may occur via differential sensitivity of presynaptic $GABA_B$ receptors at excitatory thalamocortical–stellate cell synapses versus inhibitory fast-spiking stellate cell synapses perhaps because of divergence in subunit composition and/or efficacy of coupling to inhibition of calcium channels that trigger neurotransmitter release. However, we observed minimal difference in the half-maximal inhibitory concentration for baclofen in inhibiting neurotransmission at either synapse (Supplementary Fig. 5). Thus, at any given concentration of baclofen, and hence presumably GABA, the similar extent of inhibition at these respective synapses cannot explain the observed synapse-specific modulation upon NGFC activity. Differential local GABA accumulation upon afferent stimulation selectively gates excitatory versus inhibitory inputs onto principal cells of the amygdala via presynaptic $GABA_B$ receptor activation even though both synapses can be regulated by endogenous agonist activation of this receptor[13]. A similar explanation may be possible for the circuit selectivity observed here, and a nonuniform GABA transient after NGFC activity could result in varying extent of presynaptic $GABA_B$ receptor activation at different synapses. GABA uptake mechanisms shape the spatiotemporal range of GABA. Here we showed under control conditions that NGFC activity resulted in reduction of thalamic-evoked FFI that is potentiated after GAT-1–mediated uptake block. In contrast, no similar reduction was noted in thalamic excitation of stellate cells. GAT-1 is predominantly expressed at presynaptic structures and to a lesser extent astroglial processes[14], whereas GAT-3, another major CNS GABA transporter, is exclusively expressed in the latter[14]. The GABA transient after NGFC activity in the vicinity of excitatory thalamocortical–stellate cell synapses versus inhibitory fast-spiking stellate cell synapses may significantly vary (because of local differences in uptake capacities at these synaptic locations) resulting in varying extents of presynaptic $GABA_B$ receptor activation. However, this possibility is unlikely because we demonstrated a lack of modulation of thalamocortical–stellate cell synapses by NGFC activity under conditions where both GAT-1 and GAT-3 were

simultaneously blocked (Supplementary Fig. 6). Although this is a speculation, a nonuniform distribution of release sites in the dense axonal plexus could result in a more spatially restricted mode of NGFC-mediated GABA release. In addition, the NGFC-mediated GABA transient may be influenced by varying degrees of tortuosity owing to structural differences between thalamocortical excitatory versus intracortical inhibitory synapses. Future anatomical studies, including detailed electron microscopy analyses, will be required to investigate these possibilities. Recently, the view that interneurons embed themselves in cortical circuits with precise connectivity rules has been challenged[15]. NGFCs have been classically thought to provide spatially nonselective inhibition. However our data demonstrate a synapse-specific modulation upon NGFC activity that suggests a more restricted mode of GABA transmission than previously envisioned. This selectivity bestows a new role for NGFCs in regulating integration time window that occurs via a distinct mechanism to the previously reported dynamic regulation of integration time window observed during trains of thalamic stimuli[2]. The interplay between these divergent modulatory routes would serve to enhance and/or fine-tune the transformation of the thalamic–layer IV circuitry from one that has temporal precision for faithful encoding of sensory information to one that has greater integrative properties perhaps more permissive for synaptic plasticity and ongoing refinement of receptive fields.

ONLINE METHODS

Experiments with animals

All experiments were conducted in accordance with animal protocols approved by the US National Institutes of Health.

Electrophysiology

Thalamocortical slices were prepared as described previously[16] from either *5HT$_{3A}$R-GFP* (Mutant Mouse Regional Resource Center) or NPY–humanized Renilla GFP (NPY-hrGFP; The Jackson Laboratory) transgenic mice aged P10–P14. Slices were perfused with an extracellular solution of the following composition: 119 mM NaCl, 2.5 mM KCl, 1 mM NaH_2PO4, 26.2 mM $NaHCO_3$, 11 mM glucose, 1.3 mM $MgSO_4$ and 2.5 mM $CaCl_2$, 50 μM D-AP5 saturated with 95% O_2/5% CO_2, pH 7.4 at 31–33 °C. GFP+ cells in a thalamic connected layer IV barrel were visualized using a combination of infrared illumination with differential interference contrast and fluorescence microscopy. Current-clamp recordings from GFP^+ cells possessing small, round somata in a thalamically connected layer IV barrel were performed. Internal solution for current clamp recordings had the following composition: 130 mM K-$MeSO_4$, 10 mM NaCl, 10 mM HEPES, 0.6 mM EGTA, 2 mM Mg-ATP, 0.3 mM Na-GTP and 3 mg/ml biocytin, pH 7.3; 280–290 mOsm. A series of current steps (typically −80 pA to +120 pA in 10-pA steps; 750 ms) were used to ascertain passive membrane and firing properties. A population of layer IV GFP^+ cells exhibited a characteristic depolarizing ramp and late-spiking phenotype upon subthreshold and rheobase current injections, respectively (Fig. 1d). To examine the properties of late-spiking interneuron synaptic output, paired recordings were performed with neighboring stellate cells in an approximate radius of 50 μm (Supplementary Fig. 2). Stellate cells were voltage-clamped with a high Cl^- internal solution of the following composition: 135 mM CsCl, 8

mM NaCl, 10 mM HEPES, 0.6 mM EGTA, 4 mM Mg-ATP, 0.3 mM Na-GTP and 5 mM QX-314Cl pH 7.3; 280–290 mOsm. GABA receptor–mediated unitary IPSCs mediated by late-spiking interneurons were elicited by a brief suprathreshold current injection (typically 600–900 pA; 5 ms). The unitary IPSCs mediated by interneurons with a depolarizing ramp and late-spiking characteristics were typical of those observed for NGFCs previously described (Supplementary Fig. 2) Therefore, for the remainder of the study the membrane response to subthreshold and rheobase current injections of layer IV GFP^+ cells was routinely tested and only those cells with a depolarizing ramp and late-spiking phenotype were used for subsequent analyses.

Simultaneous recordings between NGFCs and stellate cells were used to test the effect of NGFC firing on thalamic evoked FFI. NGFCs were current-clamped using the K-$MeSO_4$-based internal solution described above and stellate cells were voltage-clamped using a Cs-$MeSO_4$ solution of the following composition: 130 mM Cs-$MeSO_4$, 5 mM NaCl, 10 mM HEPES, 0.6 mM EGTA, 2 mM Mg-ATP, 0.3 mM Na-GTP and 5 mM QX-314Cl, pH 7.3; 280–290 mOsm. Feed-forward IPSCs on stellate cells (voltage-clamped at 0 mV, the reversal potential for AMPA receptor–mediated currents) were evoked at a frequency of 0.1 Hz using a bipolar stimulating electrode placed in the ventrobasal thalamus. A near minimal stimulus intensity that was sufficient to evoke FFI was used (25–100 μA; 0.1 ms). Feed-forward IPSC peak amplitude was monitored for a baseline period lasting 1.5 min after which, GABA transmission from NGFCs was elicited by three suprathreshold current injections (600–900 pA; 5 ms; 20 Hz) that preceded the thalamic stimulation by 80 ms. Feed-forward IPSC peak amplitude was continually monitored during NGFC firing for 3.5 min after which NGFC firing was switched off by ceasing the current injections and feed-forward IPSCs peak amplitudes were monitored for a final 1.5 min. The same protocol was used to test the effects of NGFC firing on thalamic-evoked EPSC amplitudes on stellate cells except that these cells were voltage-clamped at −70 mV (close to the calculated ECl^- of −66 mV). To test the effects of NGFC firing on thalamic-evoked EPSC amplitudes on fast-spiking interneurons, simultaneous recordings from NGFC and fast-spiking interneurons were performed. To facilitate targeting of both these interneuron subtypes we created a ‘double’ transgenic mouse. The Nkx2.1-cre–expressing mouse line (Ai14; The Jackson Laboratory) was initially crossed with a *tdTomato* reporter–containing mouse line (Ai14; The Jackson Laboratory). In this crossed mouse line, PV-expressing, fast-spiking inter-neurons, that are predominantly responsible for thalamic-evoked FFI in layer IV barrel cortex, are positive for tdTomato by virtue of the presence of *Nkx2-1* promoter-driven Cre activity in these interneurons during development[17]. We subsequently crossed this line with the mouse expressing NPY-hrGFP, and targeted $tdTomato^+$ and GFP^+ cells located within a single thalamic connected layer IV barrel for subsequent electrophysiological analyses (Fig. 2a). We carefully ensured that simultaneously recorded layer IV GFP^+ and $tdTomato^+$ cells demonstrated clear late-spiking (Fig. 1d) and fast-spiking, nonaccomodating (Fig. 2c) phenotypes before beginning the experiment. Fast-spiking interneurons were voltage-clamped at −70 mV, and thalamic-evoked EPSC amplitudes were monitored under baseline conditions, during NGFC firing and after firing was switched off as previously described. All values of *n* cited in the manuscript refer to the number of recorded cells (either single or

dual recordings). Each group of experiments were performed from at least two separate mice.

All electrophysiological recordings were made using a Multiclamp 700A amplifier (Molecular Devices). Signals were filtered at 4 kHz, digitized at 10 kHz and stored on computer using PClamp 9.0 software (Molecular Devices). All drugs and reagents were obtained from Sigma unless otherwise stated. D-APV, SKF89976A, (2S)-3-[[(1S)-1-(3,4-Dichlorophenyl)ethyl]amino-2-hydroxypropyl](phenylmethyl) phosphinic acid (CGP55845A), baclofen and (1,2,5,6-Tetrahydropyridin-4-yl) methylphosphinic acid (TPMPA) were purchased from Tocris Bioscience.

Modeling of thalamic-evoked conductance on stellate cells

The time course of experimentally determined thalamic-evoked feed-forward IPSCs and EPSCs on stellate cells was measured. The 20–80% rise time and τ_{decay} of the thalamic evoked feed-forward IPSCs on stellate cells were 1.92 ± 0.2 ms and 15.1 ± 2 ms, respectively (n = 5). The 20–80% rise time and τ_{decay} of the thalamic evoked EPSC were 1.23 ± 0.2 ms and 5.5 ± 1.2 ms, respectively; n = 7). As the driving forces for the outward feed-forward IPSCs and inward EPSCs were essentially the same under our experimental conditions, the relative magnitudes of the conductances equaled those of the underlying currents. Using these parameters described above, synaptic conductance profiles (g_{syn}) for feed-forward inhibitory and direct monosynaptic excitatory conductance on stellate cells were both described by the following:

$$g_{\mathrm{syn}}(t) = f k (1 - e^{-t/\tau_{\mathrm{decay}}})\,(e^{-t/20-80\%\mathrm{rise}})$$

where f is a scaling factor and k is a constant.

We have previously shown[10] that the mean value of the experimentally determined thalamic-evoked ratio between the feed-forward IPSC and EPSC amplitudes in stellate cells (measured under conditions where both currents had equivalent driving forces) at similar developmental time point used in this study was 3.8. The k constant value was set to 0.0533 and −0.0179 for the feed-forward IPSG and EPSG, respectively. With the rise and decay parameters described above, this resulted in peak amplitudes of 3.8 and −1 for the feed-forward IPSG and EPSG, respectively, thus reproducing the experimentally determined ratio of these components following thalamic stimulation. The f scaling factor for both conductances was initially set to 100. The onset of the disynaptic feed-forward IPSCs and monosynaptic were 5.34 ± 0.2 ms (n = 5) and 3.35 ± 0.4 ms (n = 7), respectively. Therefore the onset of feed-forward IPSG relative to the EPSG on stellate cells was delayed by the difference of these mean values that is, 1.99 ms. Using a custom written procedure in IGOR (Wavemetrics) the peak amplitudes of the feed-forward IPSG and EPSGs were scaled (by altering k, the scaling factor) according to the experimentally determined mean change (percentage of baseline) in feed-forward IPSC and EPSC peak amplitudes for each time point of the experiment (Fig. 2j and Supplementary Fig. 4a; that is 0.1-Hz thalamic-evoked stimulation; 1.5 min baseline, 3.5 min while NGFC firing and 1.5 min after NGFC firing was switched off; 6.5 min total = 40 time points). The feed-forward IPSG and EPSG

modeled for each of these time points were then linearly summed and the duration of integration time window determined (Supplementary Fig. 4d).

Immunocytochemistry

We obtained 50 μm frozen thalamocortical tissue sections from fixed, perfused *5HT$_{3A}$R-GFP* or *NPY-hrGFP* transgenic mice and performed immunocytochemcial staining as previously described[18]. Polyclonal anti-VGlut2 (1:1,000 dilution, cat. #AB2251) and polyclonal anti-Parvalbumin (1:5,000, cat. #PV 25) were obtained from EMD Millipore and Swant, respectively.

Statistical analyses

As no assumption was made as to the distribution of data generated, we routinely used a nonparametric statistical analyses via two-tailed Mann-Whitney *U*-test. Statistical significance is indicated as $*P < 0.05$ or $**P < 0.01$. All grouped data in the manuscript is either stated or plotted as mean values ± s.e.m.

Supplementary Material

Refer to Web version on PubMed Central for supplementary material.

Acknowledgments

We thank J. Isaac for comments, and M. Craig for the IGOR procedures used to automate analyses of the modeling data. This work was supported by the National Institute of Child Health and Human Development and National Institute of Neurological Disorders and Stroke Intramural Programs.

References

1. Cruikshank SJ, Lewis TJ, Connors BW. Nat Neurosci. 2007; 10:462–468. [PubMed: 17334362]
2. Gabernet L, Jadhav SP, Feldman DE, Carandini M, Scanziani M. Neuron. 2005; 48:315–327. [PubMed: 16242411]
3. Bruno RM, Sakmann B. Science. 2006; 312:1622–1627. [PubMed: 16778049]
4. Lee S, Hjerling-Leffler J, Zagha E, Fishell G, Rudy B. J Neurosci. 2010; 30:16796–16808. [PubMed: 21159951]
5. Olah S, et al. Nature. 2009; 461:1278–1281. [PubMed: 19865171]
6. Tamas G, Lorincz A, Simon A, Szabadics J. Science. 2003; 299:1902–1905. [PubMed: 12649485]
7. Karayannis T, et al. J Neurosci. 2010; 30:9898–9909. [PubMed: 20660272]
8. Szabadics J, Tamas G, Soltesz I. Proc Natl Acad Sci USA. 2007; 104:14831–14836. [PubMed: 17785408]
9. Manko M, Bienvenu TC, Dalezios Y, Capogna M. Physiol. 2012; 590:5611–5627.
10. Chittajallu R, Isaac JT. Nat Neurosci. 2010; 13:1240–1248. [PubMed: 20871602]
11. Gonzalez-Burgos G. Adv Pharmacol. 2010; 58:175–204. [PubMed: 20655483]
12. Schwenk J, et al. Nature. 2010; 465:231–235. [PubMed: 20400944]
13. Pan BX, et al. Neuron. 2009; 61:917–929. [PubMed: 19324000]
14. Vitellaro-Zuccarello L, Calvaresi N, De Biasi S. Cell Tissue Res. 2003; 313:245–257. [PubMed: 12898208]
15. Fino E, Packer AM, Yuste R. Neuroscientist. Aug 24.2012 10.1177/1073858412456743
16. Agmon A, Connors BW. Neuroscience. 1991; 41:365–379. [PubMed: 1870696]
17. Xu Q, Tam M, Anderson SA. J Comp Neurol. 2008; 506:16–29. [PubMed: 17990269]

18. Belachew S, et al. J Cell Biol. 2003; 161:169–186. [PubMed: 12682089]

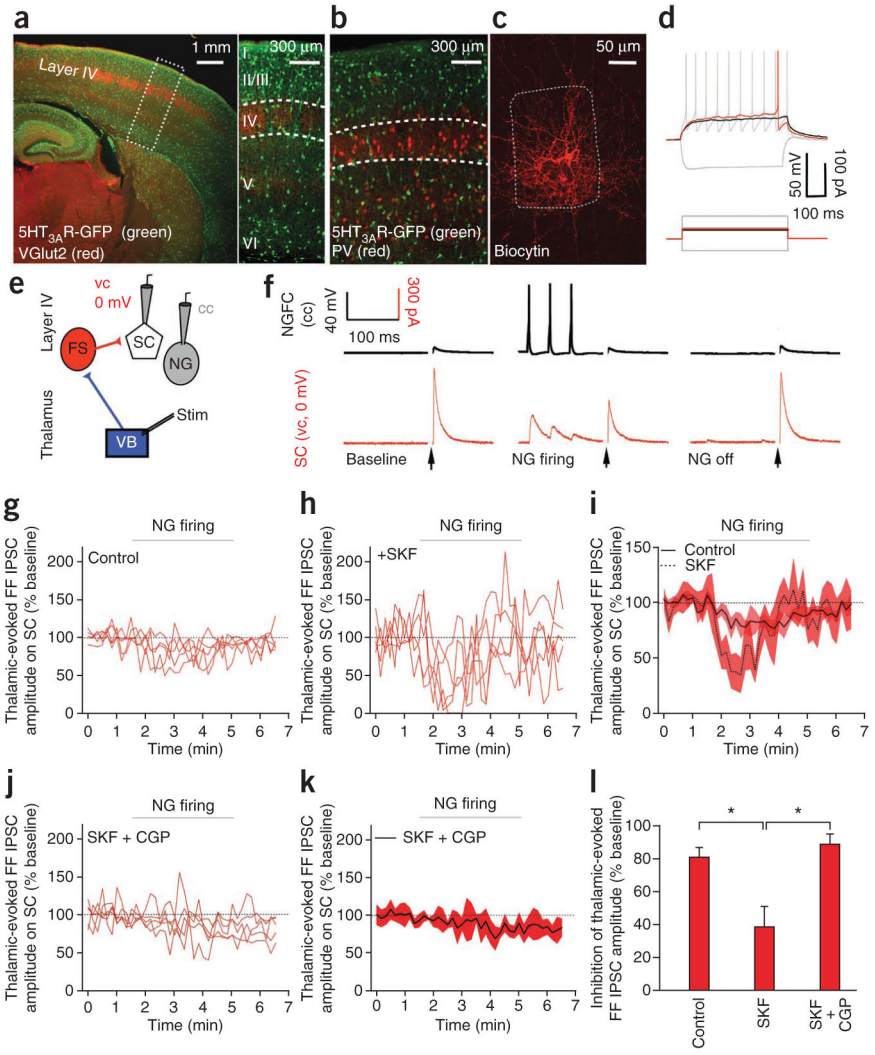

Figure 1.

Layer IV NGFC activity inhibits the canonical thalamic-evoked FFI via $GABA_B$ receptor activation. (**a**) Fluorescence image of a thalamocortical slice (left) of a mouse expressing $5HT_{3A}$R-GFP (layer IV delineated with VGlut2 immunostaining). Magnification (right) of the boxed area. (**b**) Image of $5HT_{3A}$R-GFP+ cells, stained for PV. Dashed region indicates a single layer IV barrel. (**c**) Dense axonal arborization of a biocytin-filled layer IV $5HT_{3A}$R-GFP+ cell. (**d**) Depolarizing ramp (black) and late spiking (red) of $5HT_{3A}$R-GFP+ cell at subthreshold and rheobase current injections, respectively. Gray depicts membrane responses to hyperpolarizing and 2× rheobase current injections. (**e**) Dual NGFC and stellate cell (SC) whole-cell recording configuration. cc, current clamp; FS, fast-spiking interneuron; NG, neurogliaform cell; VB, ventrobasal thalamus; vc, voltage clamp. (**f**) Single-trace examples of simultaneous current-clamp and voltage-clamp recording in an NGFC (black) and an SC (holding potential (V_h) = 0 mV; red), respectively. Left, middle and right traces are traces at baseline, during NGFC firing and after NGFC firing was turned off, respectively. Arrows denote thalamic stimulation. (**g**,**h**) Individual data showing feed-forward (FF) IPSC amplitude on SCs in control conditions (n = 5; **g**) and in presence of

GAT-1 block by 25 μM SKF-89976A (n = 5; **h**). (**i**) Pooled data of experiments depicted in **g** and **h**. (**j**,**k**) Individual (**j**) and pooled (**k**) data showing feed-forward IPSC amplitude on SCs in presence of GAT-1 uptake block (25 μM SFK-89976A) and $GABA_B$ receptor antagonism (10 μM CGP55845A; n = 5). (**l**) Summary graph of reduction in FFI amplitude 1 min after onset of NGFC firing (n = 5, $P < 0.05$). Shaded areas in **i**,**k** and error bars in **l** denote s.e.m.

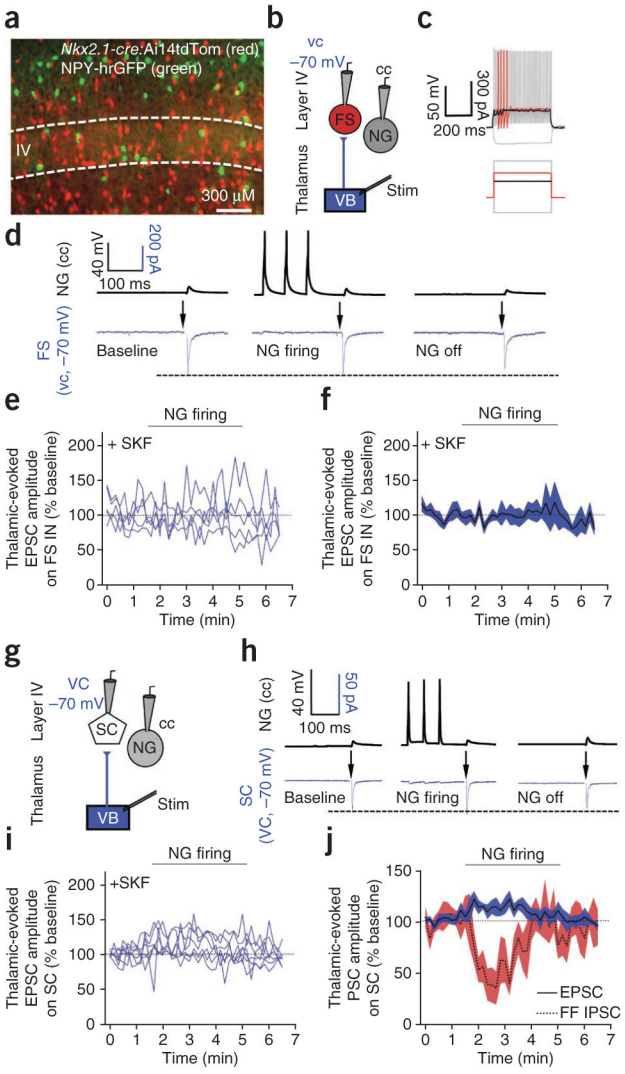

Figure 2.

NGFC activity does not affect thalamic-evoked excitatory input onto layer IV fast-spiking interneurons or stellate cells. (**a**) Fluorescence image of layer IV in a transgenic mouse expressing NPY-hrGFP and with *Nkx2.1-cre* activity reported by *loxP*-flanked tdTomato (Ai14 mouse line). (**b**) Dual NGFC and fast-spiking interneuron whole-cell recording configuration. (**c**) Representative firing pattern of fast-spiking interneurons. (**d**) Single-trace examples of simultaneous current-clamp and voltage-clamp recording in a NGFC (black) and a fast-spiking interneuron (V_h) = −70 mV; blue), respectively. Arrows denote thalamic stimulation. (**e**,**f**) Individual (**e**) and pooled (**f**) data showing thalamic-evoked EPSC amplitude on fast-spiking interneurons in presence of GAT-1 block by 25 µM SKF-89976A (n = 5). (**g**) Dual NGFC and stellate cell (SC) whole-cell recording configuration. (**h**) Single-trace examples of simultaneous current-clamp and voltage-clamp recording in a NGFC (black) and SC (V_h = −70 mV; blue), respectively. Arrows denote thalamic stimulation. (**i**,**j**) Individual (**i**) and pooled (**j**) data showing EPSC amplitude on SCs at baseline, during and after NGFC firing in presence of GAT-1 block by 25 µM SFK-89976A (n = 7). PSC,

postsynaptic current; FF, feed-forward. Red trace in **j** is a replot of the data shown in Figure 1i. Shaded areas in **f** and **j** denote s.e.m. Dotted lines in **d** and **h** indicate peak thalamic-evoked EPSC amplitude during baseline